

Structural-relaxation-induced bond length and bond angle changes in amorphized Ge

C. J. Glover and M. C. Ridgway

Department of Electronic Materials Engineering, Australian National University, Canberra, Australia

K. M. Yu

Materials Science Division, Lawrence Berkeley National Laboratory, Berkeley, California 94720

G. J. Foran

Australian Nuclear Science and Technology Organisation, Menai, Australia

D. Desnica-Frankovic

Physics Department, Rudjer Boskovic Institute, Zagreb, Croatia

C. Clerc

Centre de Spectrometrie Nucleaire et de Spectrometrie de Masse, Centre National de la Recherche Scientifique, Orsay, France

J. L. Hansen and A. Nylandsted-Larsen

Institute of Physics and Astronomy, Aarhus University, Aarhus, Denmark

(Received 5 June 2000; revised manuscript received 17 October 2000; published 31 January 2001)

Low-temperature structural relaxation in amorphized Ge has been characterized by extended x-ray-absorption fine-structure spectroscopy and Raman spectroscopy. A relaxation-temperature-dependent decrease in the mean value and asymmetry of the interatomic distance distribution has been shown to accompany the well-documented reduction in bond angle distribution. While the initial, as-implanted state of amorphous Ge was ion-dose *dependent*, relaxation at 200 °C yielded a common ion-dose-*independent* interatomic distance distribution. The heat release upon structural relaxation due to reductions in both bond length and bond angle distortion was calculated separately and the former exhibited an ion-dose dependence. The results provide compelling support for the defect annihilation model of structural relaxation and imply that the heat release upon structural relaxation should be implant-condition dependent.

DOI: 10.1103/PhysRevB.63.073204

PACS number(s): 61.43.Dq, 61.10.Ht, 61.72.Tt

Amorphous semiconductors have stimulated great interest during the past century yet a definitive microscopic understanding of these materials is still lacking. For example, though preparation conditions and thermal history influence the structure of an amorphous semiconductor, the atomic-scale nature of such structural differences has not been elucidated. Conceptually, the minimum-energy configuration of the amorphous state is a fully coordinated, continuous random network¹ (CRN) while the preparation-specific structural fluctuations described above are considered higher-energy variants, potentially containing defects, impurities, and/or voids. Structural relaxation is necessary to attain the minimum-energy configuration, as potentially mediated by thermally-induced topological reorganization and/or defect annealing and accompanied by changes in the vibrational, structural, and thermodynamic properties. Structural relaxation has been observed in the amorphous semiconductors Si,^{2,3} Ge,^{3,4} and InP (Ref. 5) and was first considered a reorganization of the matrix to minimize bond angle strain and thus, the free energy of the amorphous network.^{6,7} An alternative interpretation suggested that relaxation is a local phenomenon, attributable to pointlike defect annihilation in the amorphous phase.² This view is supported by a recent theoretical study;⁸ however, others have suggested that structural relaxation is a more diverse process, potentially involving many different mechanisms.⁹ The use of a variety of different computational frameworks in theoretical studies and the

lack of microstructural data from experimental studies thus necessitates further, refined investigation.

In amorphous Ge (*a*-Ge), structural relaxation has been characterized with many techniques, including differential scanning calorimetry (DSC),⁴ Raman spectroscopy,³ infrared spectroscopy,¹⁰ x-ray diffraction,¹¹ and extended x-ray-absorption fine-structure spectroscopy (EXAFS).^{12,13} Upon relaxation, a heat release of ~ 6 kJ/mol (Ref. 4) (or equivalently, half of the crystallization enthalpy) was measured with DSC, while Raman spectroscopy revealed a temperature-dependent reduction in the width of the bond angle distribution.³ EXAFS experiments with sputtered¹² and ion-implanted¹³ samples demonstrated that structural relaxation resulted in local reordering as manifested by a reduction in the Debye-Waller factor (σ^2), or equivalently, the mean-square relative displacement of the interatomic distance distribution. In all previous studies, the influence of the *initial, as-implanted* structure and the potential presence of non-Gaussian disorder on the extent of structural relaxation have not been considered. Herein, we present high-resolution EXAFS measurements complemented with Raman spectroscopy data of the thermally-induced structural relaxation of *a*-Ge. We show that structural relaxation is manifested by reductions in *both* the bond length and bond angle distributions and calculate the heat release associated with each component. Furthermore, we show that the extent of structural relaxation in *a*-Ge produced by ion implantation is de-

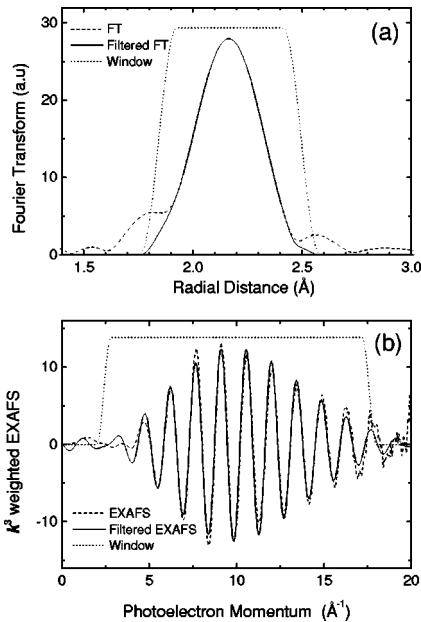


FIG. 1. (a) EXAFS and (b) Fourier-transformed spectra for *a*-Ge implanted with $1e16$ Ge ions/cm².

pendent on the extent of disorder in the as-implanted structure.

We have utilized the processing methodology described in Refs. 14 and 15 to prepare void-free, homogeneous *a*-Ge films for transmission EXAFS measurements. Crystalline Ge layers deposited by molecular-beam epitaxy were amorphized with a multiple-energy Ge ion-implantation sequence (1, 3, and 6.1 MeV) at -196 °C. The ion doses were selected to yield a constant value of energy deposition in vacancy production¹⁶ (EDVP) over the extent of the Ge layer (2 μ m). Note that the given low-temperature implant conditions did not yield porous material as consistent with previous reports.¹⁷ For the Raman measurements, bulk Ge wafers were implanted with 500-keV Ge ions with the ion doses scaled to yield a similar value of EDVP as utilized for EXAFS measurements. First-order Raman spectra were obtained in vacuum with a DILOR Z-24 triple spectrometer by excitation with the 514.5-nm line from an Ar-ion laser. Annealing was performed for 1 h in a N₂ ambient with a temperature accuracy of ± 5 °C. Transmission EXAFS measurements at the Ge *K* edge were performed at 12 K on beamlines 2-3 and 4-3 of the Stanford Synchrotron Radiation Laboratory and 20-B of the Photon Factory. Complete details of the data processing will be presented elsewhere;¹⁸ however, a brief summary follows herein. EXAFS data were extracted from absorption spectra in the conventional manner¹⁹ utilizing the SPLINE code²⁰ for the interactive background subtraction. The relative energy-scale calibration was achieved by aligning each absorption edge to within 0.1 eV. The energy origin (*E*0) was set at the maximum of the absorption-edge first derivative.²¹ As shown in Fig. 1, the EXAFS data, k^3 weighted (where k is the photoelectron momentum), was Fourier transformed (FT) over the k range 2–18 \AA^{-1} using a 5% Hanning window. The back transform was calculated using an *R*-space 20% Hanning window in the range 1.77–2.58 \AA . The Fourier filtering process allowed

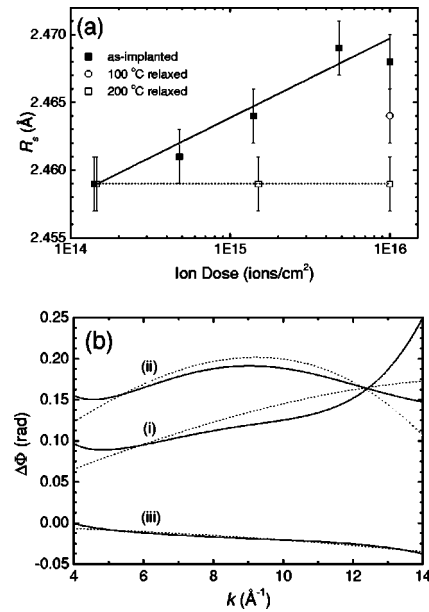


FIG. 2. (a) Nearest-neighbor bond length (R_s) as functions of ion dose and relaxation temperature and (b) phase difference ($\Delta\Phi$) for (i) as-implanted, $1.4e14$ ions/cm² and (ii) as-implanted, $1e16$ ions/cm² samples relative to the crystalline Ge standard and (iii) a relaxed, $1.4e14$ ions/cm² sample relative to an as-implanted, $1.4e14$ ions/cm² sample. Dotted lines represent third-order odd polynomial best fits (see text).

a direct extraction of the separate amplitude [$A(k)$] and phase [$\Phi(k)$] of the first-shell data used in the cumulant expansion. Relative cumulants were determined by comparing the EXAFS amplitudes and phases of the implanted samples (s) to a crystalline reference (r) fitted over the k range 4–16 \AA^{-1} . Relative cumulants $\Delta C1$ and $\Delta C3$ (where $\Delta Ci = Ci_s - Ci_r$) were obtained from a fit to the phase difference, while $\Delta C4$ and a constant containing $\Delta C2$ and N were obtained from a fit to the logarithm of the amplitude ratio.^{21,22} Absolute magnitudes of the sample cumulants were calculated from absolute values of the reference cumulants, the latter determined assuming a Gaussian interatomic distance distribution ($C3 = C4 = 0$). The XFIT code,²³ with phase and amplitude functions calculated with FEFF4.0, yielded a σ_r^2 value of 0.0018 ± 0.0003 \AA^2 . The Debye-Waller factor for *a*-Ge, σ_s^2 , was determined by adding $\Delta C2$ to σ_r^2 . The crystalline nearest-neighbor bond length was set to the x-ray diffraction standard 2.4496 \AA . The average interatomic distance for *a*-Ge and the *real* interatomic distance distribution were calculated following Dalba²¹ wherein a k -independent photoelectron mean free path of 8 \AA was assumed. Errors were determined statistically by varying *E*0 and the windowing conditions over an experimentally meaningful range.

Shown in Fig. 2 are (a) the bond length (R_s), as functions of both ion dose and annealing temperature, and (b) the phase difference ($\Delta\Phi$) as a function of photoelectron momentum. We previously reported implant-condition-dependent changes in the structural parameters of *as-implanted a*-Ge (Ref. 15) including increased R_s [Fig. 2(a)] and $C3$ values as functions of ion dose. These trends were attributed to increased disorder within the amorphous network as consistent with increased fractions of threefold- and

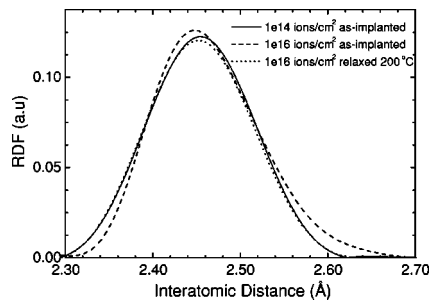


FIG. 3. Reconstructed interatomic distance distributions for as-implanted and relaxed samples as a function of ion dose.

fivefold-coordinated atoms—molecular-dynamics simulations suggest that the bond lengths of such defective configurations exceed those of fourfold-coordinated atoms.²⁴ For relaxed *a*-Ge, thermal annealing at a temperature of 200 °C yielded a common bond length value of 2.459 ± 0.002 Å independent of the ion dose. Note that no change in R_s ($\Delta R_s = -0.0007 \pm 0.001$ Å) was observed upon relaxation of the lowest dose sample, resulting in the near-zero slope of the phase difference relative to the as-implanted sample [Fig. 2(b)]. Similarly, no asymmetry in the interatomic distance distribution was measurable in either the as-implanted or relaxed states, as evidenced by the linear phase difference relative to the crystalline standard [Fig. 2(b)]. The interatomic distance distribution of the lowest dose sample was thus Gaussian. In contrast, significant asymmetry was present in the as-implanted, high dose sample as evidenced by the k^3 curvature of the phase difference relative to the crystalline standard [Fig. 2(b)]. Such asymmetry in the as-implanted state was manifested by an increased proportion of bond lengths greater than the most probable value, yielding the increased bond length shown in Fig. 2(a). Significant reductions in R_s [Fig. 2(a)], σ^2 and $C3$ were observed upon relaxation of the high dose sample ($C3$ decreased from 9.4 to $2.9 \pm 0.3e-5$ Å³).

Figure 3 shows the reconstructed interatomic distance distribution for selected samples. Note the significant reduction in asymmetry upon relaxation of the high dose sample and thereafter, the similarity of the distributions for the low dose, as-implanted and high dose, relaxed samples. For the low dose sample, the as-implanted and relaxed distributions were indistinguishable. Within experimental error, no change from the fourfold coordination was measurable for the given annealing-temperature range studied.

The temperature-dependent structural changes observed upon relaxation are consistent with the thermally-induced reduction of the threefold- and fivefold-coordinated atom fractions. Though others have previously used EXAFS to characterize structural relaxation in *a*-Ge, neither an ion-dose dependence nor the presence of non-Gaussian structural disorder were considered. Therein,¹³ relaxation at a temperature of 200 °C was manifested solely by a reduction in the Debye-Waller factor with no measurable change in bond length (to within ~ 0.01 Å) or bond angle distribution, the latter measured with Raman spectroscopy. Paesler also reported a change in the Debye-Waller factor for relaxation at 400 °C.¹² The present report has demonstrated that structural relaxation

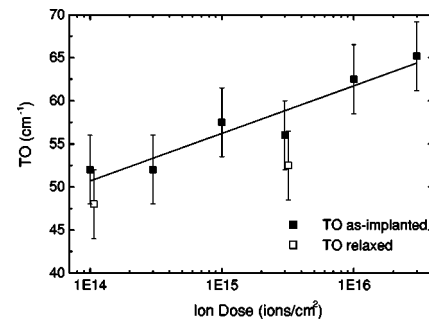


FIG. 4. FWHM of the Raman TO peak (Γ_{TO}) as functions of ion dose and relaxation temperature (200 °C). Absolute errors are shown and the relative changes measured on relaxation of the same samples are experimentally valid. For comparison with Fig. 2, the abscissa must be multiplied by ~ 3 to yield equivalent EDVP (see text).

was also accompanied by reductions in both bond length and non-Gaussian structural disorder, the extent of which were dependent on the *initial, as-implanted* state of *a*-Ge. Compared with previous reports, we attribute the greater richness of our results to improvements in the sample preparation methodology, the experimental conditions (low-temperature EXAFS in the transmission mode yielding a greater accessible k range), and the analysis methodology (explicit treatment of the non-Gaussian static disorder).

Complementary Raman measurements of as-implanted *a*-Ge samples were consistent with the conclusions derived from EXAFS measurements. Figure 4 shows the full width at half maximum (FWHM) of the TO-like band at 270 cm⁻¹ (Γ_{TO}) as a function of ion dose. For the as-implanted samples, a decrease in peak frequency (not shown) and increase in Γ_{TO} as functions of ion dose were consistent with increased disorder in the amorphous structure. Upon relaxation at a temperature of 200 °C, a reduction in Γ_{TO} of ~ 4 cm⁻¹ was measured for selected samples, independent of ion dose. Such a change was equivalent to a reduction in the bond angle distribution ($\Delta\Theta$) of $\sim 1.1^\circ$.²⁵ Others have reported comparable Γ_{TO} values for as-implanted and relaxed samples.^{3,26}

The EXAFS and Raman measurements described in the present paper have shown that the thermally induced relaxation of *a*-Ge involved reductions in *both* the bond length and bond angle distributions. The stored relaxation enthalpy in both components can be estimated. From the EXAFS measurements, the unrelaxed and relaxed interatomic distance distributions were integrated²⁷ with the potential-energy formalism of Ding and Anderson.²⁸ For the lowest dose sample, the change in the bond length distribution was negligible and thus, there was negligible calculated heat release attributable to bond length distortion. In contrast, for the highest dose sample, the calculated stored relaxation enthalpy was ~ 3.0 kJ/mol in bond length distortion upon annealing at 200 °C. From the Raman measurements, using the procedure of Tsu,²⁶ the ion-dose-independent $\sim 1.1^\circ$ change in $\Delta\Theta$ yielded a stored relaxation enthalpy of ~ 4.8 kJ/mol in bond angle distortion. *If* the two components contributing to relaxation were mutually exclusive and hence additive, the ion-dose-dependent total heat release upon relaxation was thus 4.8–7.8 kJ/mol, depending on the initial, as-implanted

state of *a*-Ge (or equivalently, ion dose). In previous measurements, a total stored relaxation enthalpy of ~ 6 kJ/mol was measured with DSC upon annealing to 400 °C.⁴

The results presented above demonstrate the influence of the initial, as-implanted structure on the extent of heat release during structural relaxation. The nonequilibrium nature of the ion implantation process yielded the ion-dose-dependent increases in both the as-implanted bond length and bond angle distributions as apparent from Figs. 2(b) and 4, respectively. Thereafter, structural relaxation was shown to result from reductions in the distortion associated with *both* parameters. Though the structural parameters measured upon annealing at 200 °C were indicative of a “relaxed” state of *a*-Ge, annealing at higher temperature may yield further relaxation. The parameters presented herein were thus not necessarily those of the minimum-energy CRN configuration. Furthermore, the relaxed state need not be defect free but may contain a critical concentration of stable defects. Thus, defining an average bond length for intrinsic *a*-Ge becomes a nontrivial task, as this value will necessarily be relaxation-state dependent. Previous measurements range from 2.45–2.47 Å (see Refs. 15 and 21 and references therein) as consistent with the results presented herein.

Our experimental results aid in identifying the nature of structural relaxation in *a*-Ge. We suggest a two-stage mechanism, similar to that described by Bouldin.¹³ The ion-dose-independent bond length measured upon annealing at ≤ 200 °C resulted from the rapid relaxation of energetically unfavorable strained bonds, associated primarily with under- and overcoordinated atoms. The reduction in bond angle distribution resulted from the relaxation of a large number of energetically more favorable, distorted bond angles. (Note that analyses of the force constants for bond stretching and bond bending indicate that the latter is energetically more favorable.²⁸) None the less, both the EXAFS and Raman data were consistent with defect annihilation as a mechanism for structural relaxation. Theoretical calculations support this as-

sertion: Kresse and Hafner²⁴ demonstrated that the presence of threefold- and fivefold-coordinated atoms yields both bond length and bond angle distortions. The subsequent removal of such defective configurations (or reduction in relative fraction) would yield a reduction in both forms of distortion, exactly as measured herein. Note that our conclusions are equally applicable to amorphous semiconductors prepared with other methods—the nonequilibrium nature of flash evaporation, sputtering, etc., can also yield structural defects that can be subsequently annihilated via structural relaxation.

In conclusion, EXAFS and Raman spectroscopies have been used to measure the structural parameters of amorphous Ge, in as-implanted and relaxed states, to characterize the thermally-induced ordering of the amorphous phase in the absence of recrystallization. In the initial, as-implanted form, the extent of both bond length and bond angle distortion was implant condition dependent. Thereafter, structural relaxation was manifested by reductions in both forms of distortion. EXAFS analysis has shown that the average bond length decreased upon relaxation to an ion-dose-independent common value. Experimental results were consistent with defect annihilation as the mechanism for structural relaxation. Furthermore, the heat release due to the reduction in both bond length and bond angle distortion was calculated separately and the former was ion-dose dependent. We thus suggest that the heat release measured by DSC upon structural relaxation of amorphous Ge should also be influenced by the implant conditions.

C.J.G., M.C.R., and G.J.F. were supported by the Australian Synchrotron Research Program, funded by the Commonwealth of Australia. K.M.Y. was supported by the Department of Energy, Office of Basic Energy Sciences. A.N.L. and J.L.H. are supported by the Danish Natural Scientific Research Council. This work was done (partially) at SSRL, which is operated by the Department of Energy, Office of Basic Energy Sciences.

-
- ¹W. H. Zachariasen, *J. Am. Chem. Soc.* **54**, 3841 (1932).
²S. Roorda *et al.*, *Phys. Rev. B* **44**, 3702 (1991).
³J. Fortner and J. S. Lannin, *Phys. Rev. B* **37**, 10 154 (1988).
⁴E. P. Donovan *et al.*, *J. Appl. Phys.* **57**, 1795 (1985).
⁵L. Cliche *et al.*, *Appl. Phys. Lett.* **65**, 1754 (1994).
⁶J. S. Lannin, *Phys. Today* **41(7)**, 28 (1988).
⁷W. C. Sinke *et al.*, *J. Mater. Res.* **3**, 1201 (1988).
⁸K. M. Beardmore and N. Gronbech-Jensen, *Phys. Rev. B* **60**, 12 610 (1999).
⁹N. Mousseau and G. T. Barkema, *Phys. Rev. B* **61**, 1898 (2000).
¹⁰E. P. Donovan *et al.*, *Nucl. Instrum. Methods Phys. Res. B* **19–20**, 590 (1987).
¹¹R. J. Temkin *et al.*, *Adv. Phys.* **22**, 581 (1974).
¹²M. A. Paesler *et al.*, *Phys. Rev. B* **28**, 4550 (1983).
¹³C. E. Bouldin *et al.*, *Phys. Rev. B* **44**, 5492 (1991).
¹⁴M. C. Ridgway *et al.*, in *Application of Synchrotron Radiation Techniques to Materials Science*, edited by S. Mimi, D. Perry, S. Stock, and L. Terminello, *Mater. Res. Soc. Symp. Proc. No. 524* (Materials Research Society, Pittsburgh, 1998), p. 309.
¹⁵M. C. Ridgway *et al.*, *Phys. Rev. B* **61**, 12 586 (2000).
¹⁶J. P. Biersack and L. G. Haggmark, *Nucl. Instrum. Methods* **174**, 257 (1980).
¹⁷B. R. Appleton *et al.*, *Appl. Phys. Lett.* **41**, 711 (1982).
¹⁸C. J. Glover *et al.* (unpublished).
¹⁹D. E. Sayers and B. A. Bunker, in *X-Ray Absorption: Principles, Applications and Techniques of EXAFS, SEXAFS and XANES*, edited by D. C. Koningsberger and R. Prins (Wiley, New York, 1988), p. 211.
²⁰P. J. Ellis, Ph.D. thesis, University of Sydney, 1995.
²¹G. Dalba *et al.*, *Phys. Rev. B* **52**, 11 034 (1995).
²²G. Bunker, *Nucl. Instrum. Methods Phys. Res.* **207**, 437 (1983).
²³P. J. Ellis and H. C. Freeman, *J. Synchrotron Radiat.* **2**, 190 (1995).
²⁴G. Kresse and J. Hafner, *Phys. Rev. B* **49**, 14 251 (1994).
²⁵For the $1e14$ ions/cm² the change in bond angle distribution was 9.5°–8.4°.
²⁶R. Tsu *et al.*, *Solid State Commun.* **54**, 447 (1985).
²⁷M. Wakagi and Y. Maeda, *Phys. Rev. B* **50**, 14 090 (1994).
²⁸K. Ding and H. C. Anderson, *Phys. Rev. B* **34**, 6987 (1986).